WALAILAK JOURNAL
http://wjst.wu.ac.th Engineering and Physical Sciences

Effects of Operating Conditions on the Ejector Characteristics and Heat Exchanger Size of Refrigeration System

Chayarnon SAENGMANEE, Kulachate PIANTHONG*, Wirapan SEEHANAM and Thanarath SRIVEERAKUL

Department of Mechanical Engineering, Ubon Ratchathani University, Ubon Ratchathani 34190, Thailand

(*Corresponding author's e-mail: Kulachate.P@ubu.ac.th)

Received: 25 August 2015, Revised: 8 January 2016, Accepted: 18 February 2016

Abstract

This study aims to investigate the operating condition effects on the characteristics of steam ejector refrigeration systems, the heat exchanger (evaporator and condenser) sizes, and the system performance. A mathematical model that co-operates with the engineering design is developed to analyze the relationships among the operating conditions, the component sizes and the system performance. A trailed system with a refrigeration capacity of 3.5 kW and operating condition ranges of 120 - 150 °C for the generator temperature, 30 - 40 °C for the condenser temperature and 5 - 10 °C for the evaporator temperature is chosen as a model case. The working fluid or the refrigerant is water (steam). In this study, it is found that varying the operating conditions strongly affects the required ejector, evaporator, and condenser sizes. The relationships obtained from this study can be used as a guideline to design an ejector refrigeration system. In addition, four different systems are analyzed to demonstrate the selection criteria for the design procedure.

Keywords: Ejector, steam, waste heat, refrigeration, heat exchanger size

Nomenclatures:

a	flow area (m^2)
a_t'	flow area per tube (m^2)
A	cross section area (m^2)
B	baffle space (m)
C	clearance (m)
C_p	specific heat (kJ/kg·K)
COP	coefficient of performance
D	diameter (m)
g	specific gravity (m/s^2)
G	mass velocity ($kg/s·m^2$)
G'	condensation loading for the horizontal tube ($kg/s·m^2$)
h	specific enthalpy (kJ/kg)
h'	heat transfer coefficient ($kW/m^2·K$)
ID	inside diameter (m)
J_H	heat transfer factor
k	thermal conductivity (W/m·K)
κ	proportionality constant
l	throat length (m)
L	length (m)
$\dot{m}$	mass flow rate (kg/s)
n	number of pass
N_t	number of tube
OD	outside diameter (m)
P	pressure (kPa)
P_T	pitch (m)
Q	heat transfer rate (kW)
R	gas constant (J/kg·K)
Rd	fouling factor
Rm	entrainment ratio
S	mixing chamber length (m)
t	water temperature (K)
T	temperature (K)
U	overall heat transfer coefficient ($kW/m^2·K$)
w	proportionality constant
W	work (kW)
x	proportionality constant
y	proportionality constant
z	proportionality constant

Abbreviations

ESDU	Engineering Sciences Data Unit
LMTD	Log Mean Temperature Difference

Greek symbols

π	Pi
ϕ	wall angle
μ	viscosity (kg/m·s)
ν	specific volume (m^3/kg)

Subscripts

1-8	refers to **Figures 1** and **Figure 2**
avg	average
c	condensation region
C	condenser
cl	clean surface
con	convergent
d	desuperheated region
dir	dirty surface
div	divergent
e	primary nozzle exit plane
eq	equivalent
E	evaporator
f	sat. liquid at condenser temperature
g	sat. vapour at condenser temperature
G	generator
i	inlet
I	inside
m	ejector throat
mix	mixed fluid
o	outlet
O	outside
p	primary
P	pump
R	area ratio
s	secondary
sh	shell
T	nozzle area ratio
t	tube
th	nozzle throat
W	wall
wi	water inlet
wo	water outlet

Introduction

In many industries, production processes are powered or operated by thermal energy. The wasted thermal energy from the process is inevitably released to the environment. The recovery or use of the waste energy would beneficial to many industries. Some favorable examples of waste energy recovery methods include preheating the combustion air, drying, steam generation, power generation, refrigeration, air conditioning, and so on.

Waste energy recycling at a low temperature (< 250 °C) can be used in alternative refrigeration systems. One possibility for recycling is the ejector refrigeration system, as it is relatively simple to construct, operate, and control compared to other systems, such as an absorption refrigeration system [1]. The ejector system is also advantageous because water can be used as the working fluid or refrigerant. Unlike the vapour compression refrigeration system, in the ejector refrigeration system, the compressor is replaced by a set of ejectors, a generator and a circulating pump. However, other components, such as a condenser, evaporator and expansion valve, are necessary. **Figures 1** and **2** show the schematic of the ejector refrigeration system and the T-s diagram of its corresponding process, respectively.

Waste energy (heat) (Q_G) is added to the generator to vaporize the working fluid. At a high pressure (P_G), the working fluid (state 1) can be used as the primary fluid ($\dot{m}_p$) for the ejector. Inside the ejector, the primary fluid at state 1 expands in the converging-diverging nozzle to a very low pressure (state 7) and entrains the low-pressure vapour (state 2) as the secondary fluid ($\dot{m}_s$) from the evaporator, where the cooling load heat (Q_E) is absorbed. At state 2, the secondary fluid is assumed to be saturated vapour. Then, the two fluids ($\dot{m}_r$) mix irreversibly and are compressed through a series of shocks in a constant chamber of the ejector at state 8. The mixed fluid is decelerated to state 3 in a diffuser of the ejector. At state 4, the liquid is assumed to be saturated liquid. A portion of the liquid ($\dot{m}_p$) accumulated in the condenser is fed to the generator by the circulating pump (state 6), and the remaining liquid ($\dot{m}_s$ at state 5) returns to the evaporator via an expansion valve.

In 1858, a condensing-type injector was invented by Henry Giffard to pump liquid water to the reservoir of steam engine boilers. In 1910, Leblanc introduced a cycle with a vapour jet ejector. His setup produced a refrigeration effect that used low-grade energy. Because steam was widely available at that

time, the so-called steam jet refrigeration systems became popular for air conditioning [2]. In the ejector refrigeration system, the ejector is the heart of the system. In this device, the kinetic energy of one fluid steam (the primary fluid) is used to entrain another fluid steam (the secondary fluid) to provide the refrigeration capacity of the system. In a well-designed ejector, the primary fluid and the secondary fluid should be fully mixed at the end of the ejector throat. In general, the ejector design is based on the effect of its operating condition and the properties of the primary and secondary fluids. The optimal ejector geometry will provide the best ejector performance under a particular operating condition. A theoretical model based on a one-dimensional analysis was first introduced by Keenan and Neuman [3]. This model is popularly used to design an ejector and evaluate its performance for many applications. Eames [4] introduced the constant rate momentum change (CRMC) method to design the ejector. Then it was developed by Milazzo and Rocchetti [5]. Moreover, some researchers [6-8] attempted to develop new mathematical models to better design the ejector and more accurately predict the ejector performance.

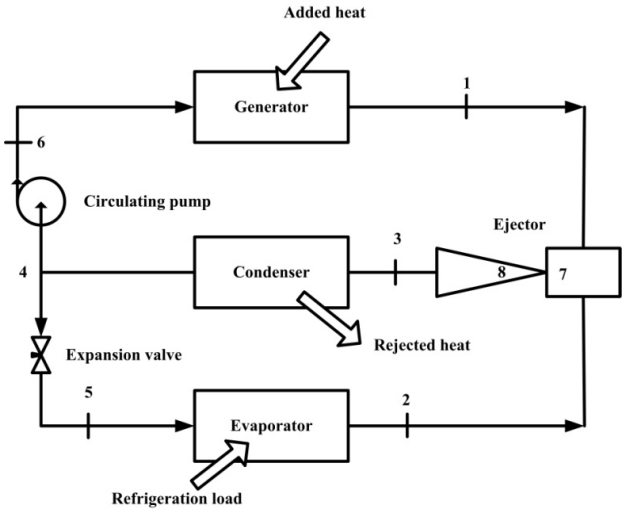

Figure 1 Schematic diagram of an ejector refrigeration system.

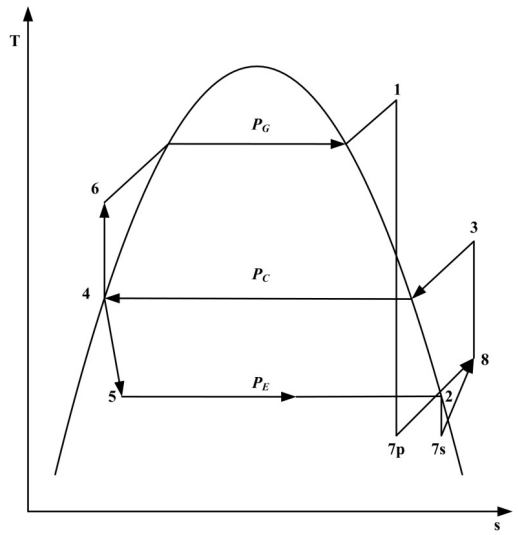

Figure 2 T-s diagram for the ejector refrigeration system.

In a refrigeration system, the performance of the ejector depends on many parameters. Therefore, researchers have focused on the effect of such parameters on the ejector performance in their reports. Huang *et al*. [9] and Sankarlal and Mani [10] found that the entrainment ratio and the coefficient of performance (COP) increased with the increase of the generator and evaporator temperatures and decreased with the increase of the condenser temperature. Then, Chen *et al*. [11] indicated that the condenser temperature has more influence than the generator and evaporator temperatures on the entrainment ratio. The critical ejector area and the entrainment ratio were discussed in the work of Selvaraju and Mani [12], which evaluated different refrigerant types. They mentioned that the ejector performed better when R134a was used as the working fluid. However, the performance of the ejector is related to both the type of working fluid and its own shape and nozzle geometry. Ruangtrakoon *et al*. [13] experimentally examined the performance of an ejector as well as the system. These authors found that the nozzle geometry has a strong effect on the ejector performance and the COP of the system. In Yapıcı's study [14], difference area ratios of ejectors were investigated, and the highest COP was only achieved when the optimal area ratio was applied. Yen *et al.* [15] tried to improve the ejector performance by using a variable throat ejector. They found that if the operating temperature varies, the variable throat ejector can be adjusted to the corresponding optimal throat area ratio. It allows the system to achieve the optimal performance. Furthermore, Butrymowicz *et al*. [16] found that the nozzle position has a very small influence on the entrainment ratio.

Moreover, a number of researchers have studied the effect of the operating conditions on the ejector geometries. Sun [17] analyzed the relationship between the ejector performance and its geometry and recommended that the ejector geometry should be variable to cope with the variations of the operating conditions to maintain an optimal performance with a constant cooling capacity. Therefore, with fixed ejector geometry, it will be difficult or impossible to always achieve the best refrigeration capacity. The results of this study showed that when the condenser temperature increased, the throat of the nozzle, the ejector throat and the length of the ejector also increased. When the boiler (the generator) temperature and the evaporator temperature increased, the nozzle throat, the ejector throat and the ejector length decreased. Rogdakis and Alexis [18] used the Munday and Bagster ejector theory to investigate the ejector design at the optimum operating condition. Their results showed that the area ratio was decreased when the primary and secondary pressures increased. Alexis [19] used a simple method to estimate the main cross sections of the steam ejector in the refrigeration system. These authors showed that the area ratio and the cross section of the secondary steam from the nozzle exit plane to the nozzle throat increased with increasing evaporator temperature. However, the cross section area of the nozzle exit plane to the nozzle throat decreased with increasing evaporator temperature.

For many years, numerical methods have been developed, particularly the computation fluid dynamics (CFD) method. Many researchers [20-23] used the CFD method to explain the flow characteristics and to predict the ejector performance. They found that the results from the CFD model were closer to the experimentally obtained actual values than the theoretical analysis results. Therefore, some researchers [24,25] used the CFD method to discover the optimal ejector geometries. Ruangtrakoon *et al*. [26] employed the CFD technique to simulate the effect of primary nozzle geometries on ejector performance. The Mach number contour lines were used to explain the mixing process occurring inside the ejector. They found that the shock's position and the expansion angle are the important parameter which influence on the ejector performance.

From the previously mentioned studies, researchers have typically focused on the operating condition effects on the dimension, shape, and performance of the ejector refrigeration system using either a mathematical model or the CFD method. However, the system component selection and the performance prediction have not been thoroughly investigated. Therefore, this paper analyzes the operating condition effects on the required sizes of the components (i.e., ejector, evaporator, and condenser) and the performance of an ejector refrigeration system. A mathematical model and the engineering design are used as the tools. The graphical relationships obtained from this study can be used as a guideline to design an ejector refrigeration system for the same operating conditions ranges. Especially, it is suitable for the system which operates in the tropical climate area because the operating conditions used to simulate are in a tropical climate. Furthermore, water with zero ozone depletion

potential and global warming potential, was selected as the refrigerant. One can also follow the example procedure to design a system that operates outside of the initial conditions of this study.

Materials and methods

Mathematical models of the ejector refrigeration system

Ejector

In this study, the ejector is firstly selected to be the constant pressure mixing (CPM) type. The principal dimensions of the steam ejector, as shown in **Figure 3**, have been estimated using the following criteria.

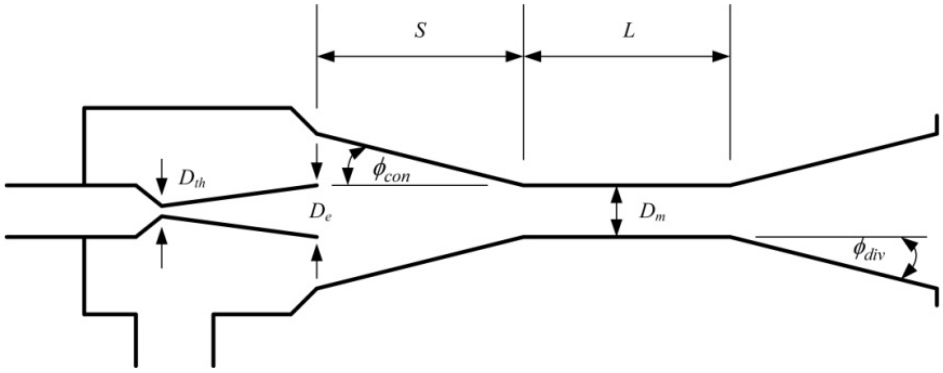

Figure 3 Principal dimensions of the steam ejector.

The ESDU [27] method is used to design the dimension and the shape of the constant pressure mixing (CPM) ejector. The required refrigeration capacity and the operating conditions (pressure and temperature of the generator, the condenser, and the evaporator) are specified as the initial conditions.

From the energy balance, the refrigeration capacity is defined as the evaporator load (Q_E) under the steady-state condition as follows;

$$Q_E = \dot{m}_s (h_2 - h_5) \tag{1}$$

According to the relationship in ESDU, the unknown parameters, which are the entrainment ratio (Rm), the nozzle area ratio (A_T) and the area ratio (A_R), are estimated in correspondence with the secondary mass flow rate ($\dot{m}_s$) from Eq. (1). The primary mass flow rate)$\dot{m}_p$(of the high-pressure steam (i.e., the refrigerant is water) from the generator is estimated according to following equation;

$$\dot{m}_p = \frac{\dot{m}_s}{Rm} \tag{2}$$

The area of the primary nozzle throat (A_{th}) is estimated according to the following equation;

$$A_{th} = \frac{\dot{m}_p \sqrt{T_p R}}{\kappa P_p} \tag{3}$$

where $\dot{m}_p$, P_p, T_p, R and κ are the primary mass flow rate, the primary pressure, the primary temperature, the gas constant and the constant value, respectively. $\kappa = 0.67$ for superheated steam.

Then, the diameter of the primary nozzle throat (D_{th}) is calculated by;

$$D_{th} = \sqrt{\frac{4A_{th}}{\pi}} \tag{4}$$

The area of the primary nozzle exit plane is calculated using the following formula;

$$A_e = A_T A_{th} \tag{5}$$

where A_T is the nozzle area ratio, which is an unknown parameter and is determined by an appropriate relationship in ESDU [27].

The area of the ejector throat is calculated by;

$$A_m = A_R A_{th} \tag{6}$$

The shape and the length of the steam ejector are determined using Eqs. (7) to (10);

$$l = 2 \text{ to } 4Dm \tag{7}$$

$$S = 10Dm - l \tag{8}$$

$$\phi_{con} = 2° \text{ to } 10° \tag{9}$$

$$\phi_{div} = 3° \text{ to } 5° \tag{10}$$

where l, S, ϕ_{con} and ϕ_{div} are the ejector throat length, the mixing chamber length, the convergent wall angle and the divergent wall angle, respectively. In this study, a CPM-type steam ejector is used as a model ejector in the analysis. The applied throat length, the convergent angle and the divergent angle are $4D_m$, 2° and 3°, respectively. These figures are obtained from the recommended ESDU coupled with the verification from the CFD simulation in our previous study [28] to achieve the best performance.

Heat exchangers

Condenser

In this study, the condenser is a shell and tube heat exchanger to cool the steam from the ejector into liquid form. This type of heat exchanger is suitable for the ejector refrigeration system. In the condensing process, the heat is removed from the steam that enters the shell and condenses into its liquid phase when it encounters the cooling water that flows in the tube. Normally, because the desuperheated and condensation processes occur in the condenser shell, they must be considered in the condenser design.

The condenser design procedure [29] is described as follows. First, the initial conditions include the standard shell and tube heat exchanger (**Table 1**), which is selected from the Tube-sheet layouts table, the condenser pressure, the working fluid (or refrigerant) and the cooling water temperatures at both the inlet and the outlet, as well as the mass flow rate of both fluids are specified. These initial conditions are used to determine the condenser dimensions.

Table 1 Condenser and evaporator details.

	Condenser	**Evaporator**
Shell side (stainless steel)		
Inside dia. (m)	0.254	0.254
Baffle space (m)	0.1016	0.1016
Tube side (Copper)		
Inside dia. (m)	0.0157	0.0157
Outside dia. (m)	0.01905	0.01905
BWG	16	16
Pith (m)	0.0254	0.0254
Number of tube	52	52
Number of pass	2	2
Flow area per tube (m^2)	0.000195	0.000195
Length (m)	1.5	1.8
Clearance (m)	0.00635	0.00635

Desuperheated region

Shell side

From the schematics in **Figures 1** and **2**, considering the energy balance around the condenser, the cooling loads in the desuperheated (Q_d) and the condensation region (Q_c) can be determined using Eqs. (11) and (12).

$$Q_d = \dot{m}_r (h_3 - h_g) \tag{11}$$

$$Q_c = \dot{m}_r (h_f - h_g) \tag{12}$$

where $\dot{m}_r$ is the refrigerant (primary and secondary steam) mass flow rate.

The enthalpy of refrigerant flow at the condenser inlet (or ejector exit), h_3, can be calculated from an energy conservation equation neglecting the kinetic energy loss, as shown in the Eq. (13);

$$h_3 = \frac{Rmh_2 + h_1}{Rm + 1} \tag{13}$$

The Log Mean Temperature Difference in the desuperheated region ($LMTD_d$) is expressed by;

$$LMTD_d = \frac{\left[(T_{C,i} - t_{wo,d}) - (T_{C,o} - t_{wi,d})\right]}{ln\left[T_{C,i} - t_{wo,d} / T_{C,o} - t_{wi,d}\right]} \tag{14}$$

where $T_{C,i}$ and $T_{C,o}$ are the refrigerant temperature at the condenser inlet and outlet, respectively. In the calculation, the refrigerant conditions at the inlet and outlet of the condenser are identically assigned to the refrigerant exit from the ejector condition and the saturated liquid state, respectively. In addition, $t_{wi,d}$ and $t_{wo,d}$ in Eq. (14) are the temperatures of the cooling water inlet and outlet in desuperheated region respectively, and can be estimated from Eqs. (11) and (12).

The refrigerant temperature at the condenser inlet ($T_{C,i}$) can be determined by using Eqs. (15) and (16);

$$T_{C,i} = T_{C,o} + \frac{h_3 + h_g}{Cp} \tag{15}$$

$$Cp = w + xT_{C,i} + yT_{C,i}^2 + zT_{C,i}^3 \tag{16}$$

where Cp is the specific heat (kJ/kmol·K) and w, x, y and z are the proportionality constants 32.24, 0.1923×10^{-2}, 1.055×10^{-5} and -3.595×10^{-9}, respectively.

The cross flow area (a_{sh}) of the refrigerant -filled shell is calculated as follows;

$$a_{sh} = \frac{ID_{sh}CB}{P_T} \tag{17}$$

where ID_{sh}, C, B and P_T are the diameters of the shell interior, the clearance, the baffle space and the tube pitch, respectively. The mass velocity in the shell side (G_{sh}) is calculated by;

$$G_{sh} = \frac{\dot{m}_r}{a_{sh}} \tag{18}$$

Then, the equivalent diameter of the shell (D_{eq}) is four times the hydraulic radius. This relationship corresponds to the area of a circle, which is equivalent to the area of a noncircular flow channel and consequently in a plane perpendicular to the flow direction. D_{eq} is specified by;

$$D_{eq} = \frac{4\left[P_T^2 - \left(\pi d_o^2 / 4\right)\right]}{\pi d_o} \tag{19}$$

where d_O is the outer diameter of the tube. Thus, the Reynolds number (Re) of the flow is calculated using the following equation;

$$Re = \frac{D_{eq}G_{sh}}{\mu} \tag{20}$$

Therefore, corresponding to Re, the heat transfer factor (J_H) is achieved by estimating the shell side heat transfer in the curve recommended by Kern [29]. Hence, the coefficient (h_O) of heat transfer around the tube is computed as follows;

$$h_O = J_H \frac{k}{D_{eq}}\left(\frac{Cp\mu}{k}\right)^{1/3} \tag{21}$$

where Cp, k and μ are the specific heat, the thermal conductivity and the viscosity of the refrigerant, respectively. These properties are averaged throughout the condenser.

Tube side

The flow area (a_t) of the tube, which is filled to the brim with cooling water, is calculated using Eq. (22).

$$a_t = \frac{N_t a_t'}{n} \tag{22}$$

where N_t, $á_t$ and n are the number of tubes, the flow area per tube and the number of passes, respectively. The mass velocity (G_t) is given in Eq. (23), where $\dot{m}$ is the mass flow rate of the cooling water in the tube.

$$G_t = \frac{\dot{m}}{a_t} \tag{23}$$

The specific heat (Cp), the thermal conductivity (k) and the viscosity (μ) of the cooling water at the average cooling water temperature in the desuperheat region are used to computed the Reynolds number (Re) and the heat transfer coefficient inside the tube (h_I). The Reynolds number (Re) of the cooling water that flows in the tube is computed from;

$$Re = \frac{ID_t G_t}{\mu} \tag{24}$$

where ID_t is the inner diameter of the tube, and μ is the viscosity of the fluid.

From the calculation of Re and the length-to-diameter ratio of the tube (L/ID_t), the heat transfer factor (J_H) associated with the tube side heat transfer curve [29] is estimated. The heat transfer coefficient (h_I) is computed from Eq. (25).

$$h_I = J_H \frac{k}{ID_t}\left(\frac{Cp\mu}{k}\right)^{1/3} \tag{25}$$

To calculate the overall heat transfer coefficient (U_{cl}) based on the outside diameter surface area, let h_{IO} be the value of h_I for the outer diameter [29].

$$h_{IO} = h_I \frac{ID_t}{OD_t} \tag{26}$$

Then, Eqs. (27) and (28) give the overall heat transfer coefficients over clean (U_{cl}) and dirty surfaces (U_{dir}), respectively, neglecting the pipe wall resistance.

$$U_{cl} = \frac{h_{IO} h_O}{h_{IO} + h_O} \tag{27}$$

$$\frac{1}{U_{dir}} = \frac{1}{U_{cl}} + Rd \tag{28}$$

where Rd is the fouling factor (Rd = 0.000176 m^2 K/W for city water or well water [30]). Hence, the heat transfer area of the desuperheating region (A_d) is computed as;

$$A_d = \frac{Q_d}{U_{dir} LMTD_d} \tag{29}$$

Condensation region

Shell side

The Log Mean Temperature Difference in the condensation region ($LMTD_c$) is expressed by;

$$LMTD_c = \frac{\left[(T_C - t_{wi,d}) - (T_C - t_{wi,C})\right]}{ln\left[T_C - t_{wi,d} / T_C - t_{wi,C}\right]} \tag{30}$$

where T_C, $t_{wi,C}$ and $t_{wi,d}$ are the refrigerant temperatures at the condenser outlet, the cooling water temperature at the condenser inlet and that at the desuperheat region inlet of the condenser, respectively.

The formula to compute the condensation loading for the horizontal tube (G') is;

$$G' = \frac{\dot{m}_r}{LN_t^{2/3}} \tag{31}$$

By initiating the heat transfer coefficient outside the tube (h_O) is assumed, the temperature (T_W) of the tube wall is computed using Eq. (32).

$$T_W = T_{avg} + \left(\frac{h_O}{h_{IO} + h_O}\right)\left(T_C - T_{avg}\right) \tag{32}$$

This temperature is used to determine the thermal conductivity (k) and the viscosity (μ) of the refrigerant.

The heat transfer coefficient (h') is calculated by;

$$h'\left[\frac{\mu^2}{k^3 \rho^2 g}\right]^{1/3} = 1.51\left(\frac{4G'}{\mu}\right)^{-1/3} \tag{33}$$

With proper iteration, the value of the heat transfer coefficient (h') from Eq. (33) satisfactorily approaches the initial assumption (h_O). In this situation, this coefficient is used in Eqs. (27) and (28) to estimate the overall heat transfer coefficients around clean (U_{cl}) and dirty (U_{dir}) surfaces. Therefore, the heat transfer area of the condensation region (A_c) is computed as [29];

$$A_c = \frac{Q_c}{U_{dir} LMTD_c} \tag{34}$$

Note that the heat transfer area of the condenser (A_C) is the sum of the heat transfer area of the desuperheat region (A_d) and the condensation region (A_c). If the condenser has a smaller heat transfer area than the standard shell and tube heat exchanger, which is initially selected, it can be used as the shell and tube heat exchanger based on the initial selection.

Evaporator

This section describes the design procedure of the evaporator [29]. A flooded evaporator or chiller is applied in this system. The calculation assigns the working fluid or refrigerant (water) flow in the shell and the chilled water flow in the tube. The design procedure is as follows. First, the initial conditions (the

refrigeration capacity (Q_E), the pressure and the temperature of an evaporator, the temperature of the inlet and outlet chilled water, the mass flow rate of the water and the shell and tube heat exchanger (shown in **Table 1**) are selected from the recommended table. Then, those conditions are used to determine the evaporator dimensions as follows.

The Log Mean Temperature Difference of the evaporator ($LMTD_E$) is computed as;

$$LMTD_E = \frac{\left[(T_E - t_{wi}) - (T_E - t_{wo})\right]}{ln\left[T_E - t_{wi}/T_E - t_{wo}\right]} \tag{35}$$

where T_E, t_{wi} and t_{wo} are the evaporator temperature, the inlet chilled water temperature and the outlet chilled-water temperature, respectively.

Tube side

The relationship between the heat transfer coefficient in the tube and the tube outer diameter (h_{IO}) is determined using Eqs. (22) - (26).

Shell side

The heat transfer coefficient outside the tube (h_o) is assumed to determine the tube wall temperature (T_W) using Eq. (36);

$$T_W = T_{avg} + \left(\frac{h_{IO}}{h_{IO} + h_O}\right)\left(T_E - T_{avg}\right) \tag{36}$$

where t_{avg} is the average temperature of the chilled water. Because the heat transfer coefficient outside the tube (h_O) is estimated from the natural circulation boiling and the sensible film coefficient curve, the difference temperature (Δt) between the wall and the water is required. If the estimated h_O is appropriately close to the assumption value, this coefficient can be applied for the next calculation step.

Finally, for the clean and dirty surfaces along the evaporator tube, the overall heat transfer coefficient can also be calculated using Eqs. (27) and (28). Hence, the heat transfer area of the evaporator (A_E) is computed as;

$$A_E = \frac{Q_E}{U_{dir} LMTD_E} \tag{37}$$

Similar to the condenser design, if the heat transfer area (A_E) in Eq. (34) is less than that of the initially selected standard shell and tube heat exchanger, the standard heat exchanger will be applied for the system.

System performance

According to the schematic diagram of the ejector refrigeration system in **Figures 1** and **2**, the heat and mass balance of the system have the following relationships;

$$Q_G = \dot{m}_p (h_1 - h_6) \tag{38}$$

$$Q_E = \dot{m}_s (h_2 - h_5) \tag{39}$$

$$Q_C = \dot{m}_r (h_3 - h_4) \tag{40}$$

$$\dot{m}_r = \dot{m}_p + \dot{m}_s \tag{41}$$

where Q_G, Q_E, and Q_C are the heat transfer rate of the generator, evaporator and condenser, respectively. $\dot{m}_p$ $\dot{m}_s$ and $\dot{m}_r$ are the primary, secondary and refrigerant mass flow rate, respectively. h_1 to h_6 are the specific enthalpies, refer to **Figures 1** and **2**.

To predict the system performance, the COP, which represents the ratio of the refrigeration capacity to the power input, is calculated by Eq. (42);

$$COP = \frac{Q_E}{Q_G + W_P} = \frac{Rm(h_2 - h_5)}{(h_1 - h_6) + \nu(P_G - P_C)} \tag{42}$$

where W_P, ν, P_G and P_C are the work of pump, specific volume and pressure of the generator and condenser. Rm is the entrainment ratio of the ejector, which is defined as follows;

$$Rm = \frac{\dot{m}_s}{\dot{m}_p} \tag{43}$$

Operating conditions

For this study, the operating conditions used to simulate the effect on the dimension, shape, and performance of the ejector refrigeration system was a tropical climate. For a tropical climate, the major obstacle is the high operating temperature at the condenser. Because the cooling water (or air) temperature that was used to transfer the heat from the refrigerant is high and it directly effects on the dimension, shape, and performance of the system. Furthermore, water with zero ozone depletion potential and global warming potential, was used as the refrigerant. Hence, the relationships obtained from this study can be used as a guideline to design an ejector refrigeration system which uses water as a refrigerant and operates in a tropical climate area. **Table 2** shows the operating conditions of this study.

Table 2 Operating conditions.

Simulation conditions	
Refrigeration capacity (kW)	3.5
Generator temperature (°C)	120 - 150
Condenser temperature (°C)	30 - 40
Evaporator temperature (°C)	5 - 10
Refrigerant	Water
Cooling water inlet the condenser (°C)	25
Cooling water flow rate (kg/s)	0.567

Results and discussion

Effect of the generator temperature

From the calculation, the effect of the generator temperature on the performance characteristics of the steam ejector refrigeration system, when the other operating conditions are fixed, is graphically presented in **Figures 4 - 7**.

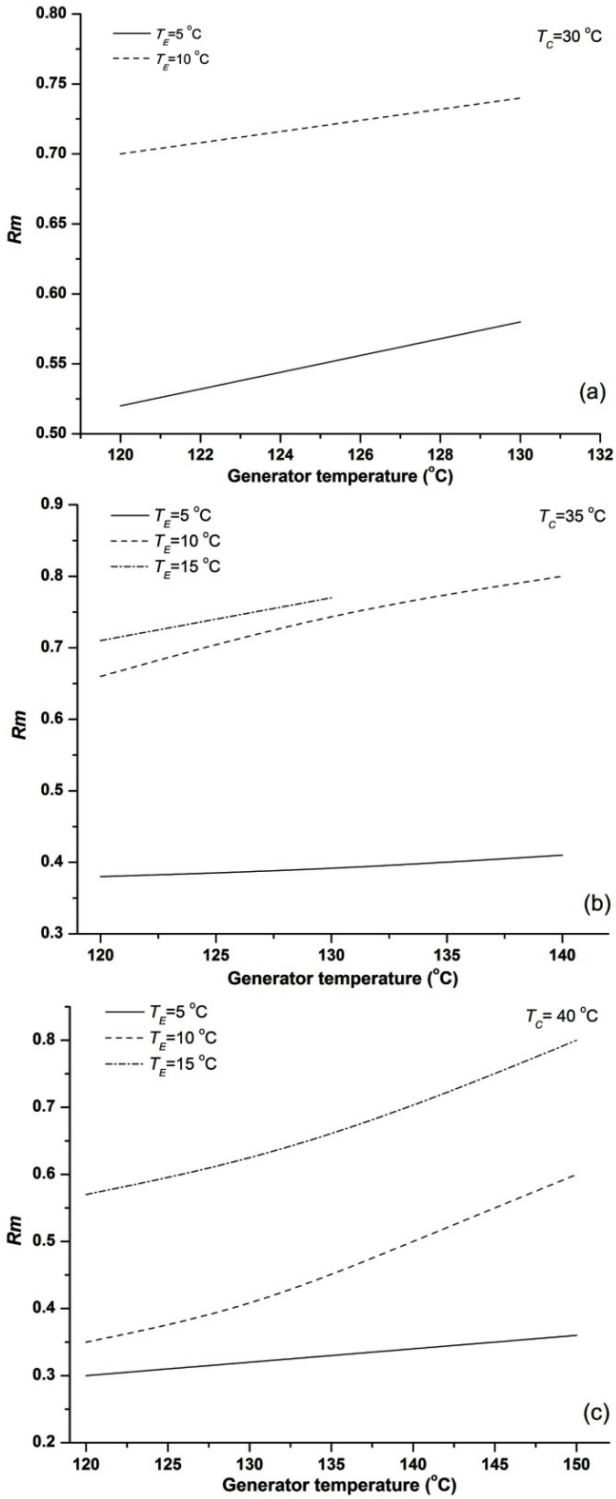

Figure 4 Effect of operating conditions on the entrainment ratio with the condenser temperature of (a) 30 °C, (b) 35 °C and (c) 40 °C.

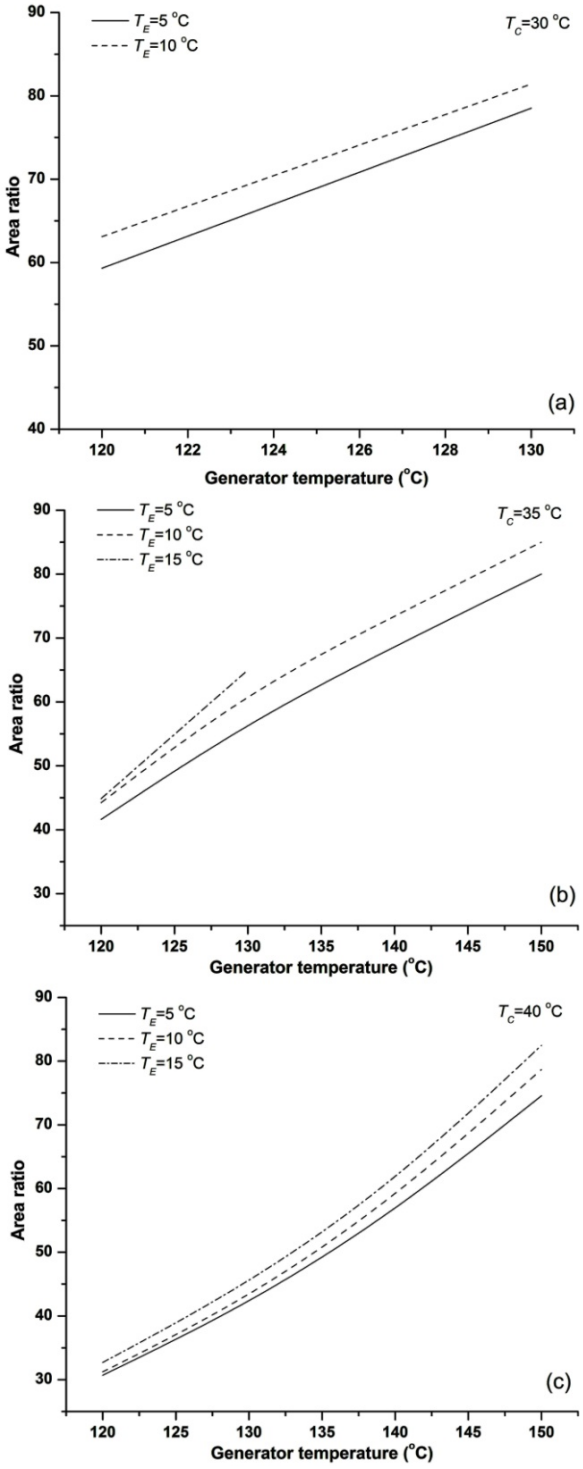

Figure 5 Effect of operating conditions on the area ratio with condenser temperature of (a) 30 °C, (b) 35 °C and (c) 40 °C.

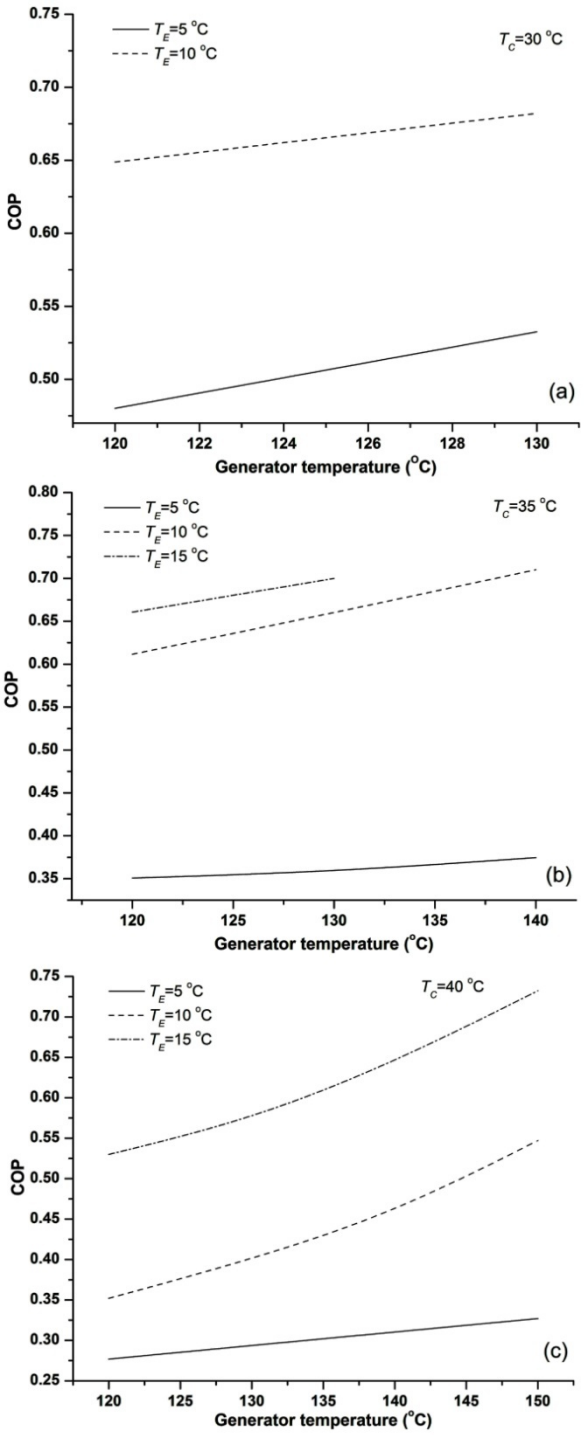

Figure 6 Effect of operating conditions on the COP with the condenser temperature of (a) 30 °C, (b) 35 °C and (c) 40 °C.

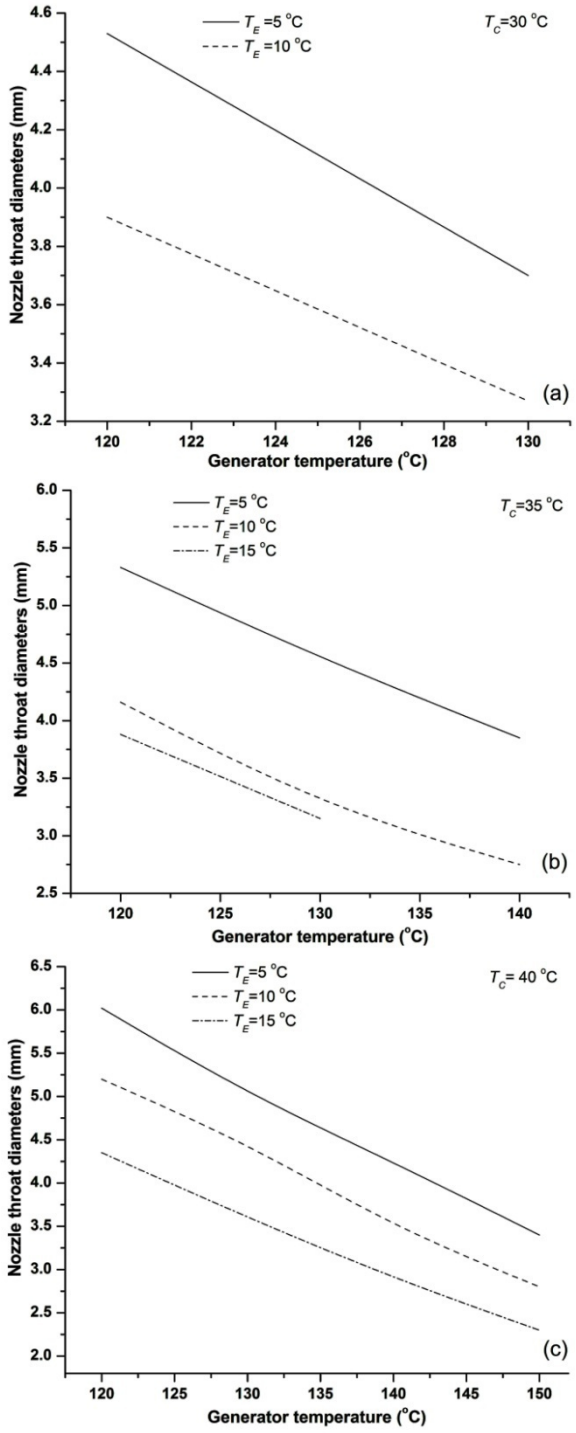

Figure 7 Effect of operating conditions on the nozzle throat diameter with the condenser temperature of (a) 30 °C, (b) 35 °C and (c) condenser temperature of 40 °C.

Figure 4 demonstrates that when the generator temperature increases, the entrainment ratio increases. Because the secondary mass flow rate is maintained at a constant rate, whereas the primary mass flow is decreased, the entrainment ratio increases. This increase causes the area ratio and the COP to increase. **Figure 5** shows that when the generator temperature increases, the area ratio increases because the primary nozzle throat decreases at a greater rate than the ejector throat. **Figures 4** and **5** reveal that at identical operating conditions, similar trends of the entrainment and the area ratios are observed, that is, the area ratio increases when the entrainment ratio increases. This result occurs because when the entrainment ratio increases, a larger cross section area is required for the mixed fluid flow [12]. Therefore, the entrainment ratio directly influences the area ratio.

Figure 6 presents the relationship between the generator temperature and the COP. It reveals that when the generator temperature increases, the COP increases because the entrainment ratio significantly increases when the generator temperature increases [31]. This result is confirmed by Eq. (42), where the COP is directly proportional to the entrainment ratio. However, the primary nozzle throat diameter decreases when the generator temperature is increased, as shown in **Figures 7a, 7b** and **7c**. Because a smaller primary mass flow rate is required to entrain the same secondary mass flow rate, the throat diameter must decrease.

Effect of the evaporator temperature

The effect of the evaporator temperature on the performance characteristics of the steam ejector refrigeration system, when the other operating conditions are maintained constant, can be predicted from **Figures 4 - 7**. **Figure 4** shows that when the evaporator temperature is increased, the entrainment ratio increases because the primary mass flow rate decreases more rapidly than the secondary flow rate. For the generator and condenser temperatures of 120 and 40 °C, respectively, the entrainment ratio at the evaporator at 5 °C is less than that at 10 and 15 °C, respectively. Similar trends are also found for the other operating conditions.

Figure 5 reveals that when the evaporator temperature increases, the area ratio increases because the primary pressure ratio is fixed and the entrainment ratio increases. Here, the primary pressure ratio is defined as the ratio of the generator pressure to the condenser pressure. **Figure 6** shows that the COP is increased when the evaporator temperature increases because the entrainment ratio increases and the enthalpy decreases more rapidly across the generator than across the evaporator. When the evaporator temperature increases, the primary mass flow rate decreases, which decreases the primary nozzle throat. **Figure 7** shows that the throat diameter is indeed decreased when the evaporator temperature increases.

Effect of the condenser temperature

Figures 4 - 7 also display the effect of the condenser temperature on the performance characteristics of the steam ejector refrigeration system when the other operating conditions are maintained at constant values.

Figure 4 reveals that when the condenser temperature increases, the entrainment ratio is decreased because the primary mass flow rate increases more rapidly than the secondary mass flow rate [6]. Hence, a larger primary nozzle throat diameter can be achieved, as shown in **Figure 7**. When the generator and evaporator temperatures are 120 and 5 °C, respectively, the throat diameter at the condenser temperature of 30, 35 and 40 °C is approximately 4.5, 5.3 and 6.0 mm, respectively.

Figure 5 shows that when the condenser temperature is increased, the area ratio decreases because the diameter of the primary nozzle throat increases but that of the ejector throat decreases. The area ratio at the condenser temperature of 30, 35 and 40 °C is approximately 63, 41 and 31, respectively, when the generator temperature is 120 °C and the evaporator temperature is 5 °C.

The COP depends on the entrainment ratio of the system. For this condition, the entrainment ratio decreases with an increase in the condenser temperature, as shown in **Figure 4**, which makes the COP decrease, as shown in **Figure 6**. When the generator and evaporator temperatures are 120 and 5 °C, respectively, the COP at the condenser temperature of 30, 35 and 40 °C are approximately 0.48, 0.35 and

0.28, respectively. According to the above results, the condenser temperature is inversely proportional to the entrainment ratio, the area ratio and the COP. However, it is directly proportional to the primary nozzle throat diameter.

Effect of the operating conditions on the condenser size

In the steam ejector refrigeration system, the condenser is used to reject the heat that is added to the system at the generator and the evaporator. Thus, the rejected-heat transfer area is a significant parameter that indicates the size and cost of the condenser. The operating conditions of the system affect the amount of rejected heat and hence the condenser size, as shown in **Figures 8** and **9**.

Figure 8 shows that the heat transfer area must slightly increase when the generator temperature is increased at constant evaporator and condenser temperatures. This requirement is necessary because the heat transfer area in the desuperheated region slightly increases, whereas that in the condensation region remains constant.

At constant generator and evaporator temperatures, it is clear that the heat transfer area of the condenser decreases when the condenser temperature increases because the Log Mean Temperature Difference (LMTD) increases, whereas the condenser load decreases, and the overall heat transfer coefficient of the condenser remains constant. The average heat transfer area of the condenser is 7.29, 3.49 and 2.37 m^2 when the condenser temperature is 30, 35 and 40 °C, respectively.

The cooling water, which is circulated to transfer the heat from the refrigeration in the condenser, also affects the heat transfer area of the condenser. **Figure 9** shows that the heat transfer area increases when the cooling-water temperature increases. The minimum and maximum heat transfer areas are between 1.6 m^2 and 3.5 m^2 when the cooling water is 15 and 30 °C, respectively.

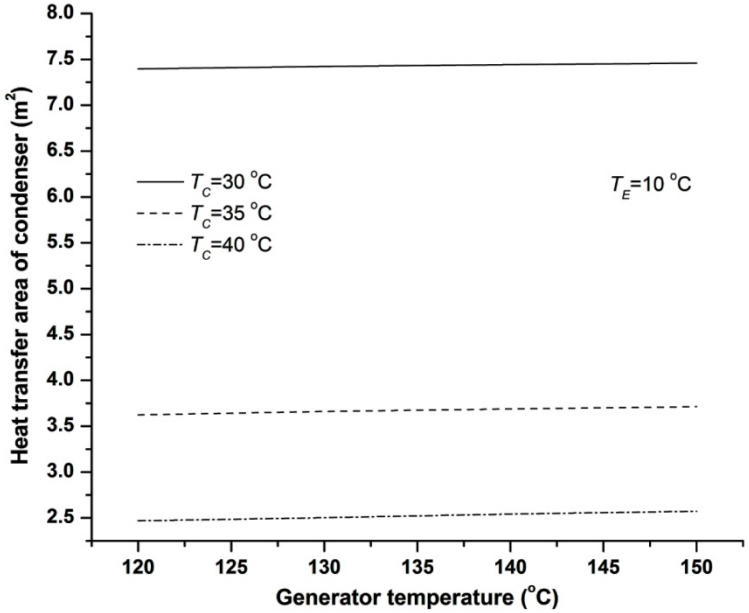

Figure 8 Effect of operating conditions on the heat transfer area of condenser.

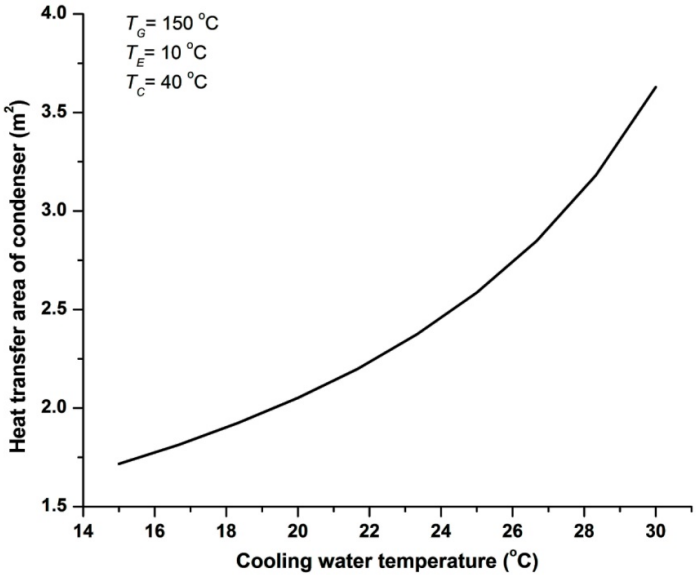

Figure 9 Effect of cooling water temperature on the heat transfer area of condenser.

Effect of the operating conditions on the evaporator size

In this study, the flooded evaporator is used to evaporate the refrigerant from a liquid to a gas by absorbing the heat from the chilled water. Similar to the condenser, the size of the evaporator corresponds to the operating conditions. **Figure 10** shows the effect of the operating conditions on the evaporator size: the heat transfer area of the evaporator increases when the refrigeration capacity increases at constant evaporator temperature and chilled water temperature. Moreover, the heat transfer area clearly increases when the evaporator temperature increases because the LMTD is decreased.

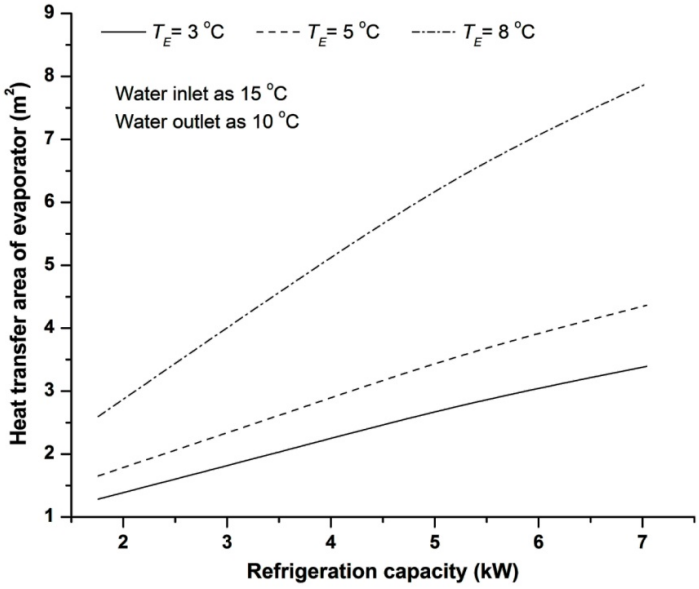

Figure 10 Effect of refrigerant capacity on the heat transfer area of the evaporator.

Selection criteria and performance prediction

In the previous section, the operating condition effects on the size of the system components (ejector, condenser and evaporator) and the system performance were analyzed and graphically presented (**Figures 4 - 10**). These figures are obtained from the initial conditions of our case of interest, which is described in **Table 2**. If the refrigeration capacity and the operating conditions are in the same ranges of **Table 2**, the equipment size can be directly selected from **Figures 4 - 10**. For example, this section shows how to select the appropriate equipment sizes using the analysis of this study.

Table 3 shows an example procedure to select the equipment size and the prediction of the system performance. The first step is to define the refrigerating capacity, the working fluid type, and the operation conditions. Then, the ejector size, the evaporator heat transfer area and the condenser heat transfer area can be obtained from the 1-D analysis results (graphical plots). The ejector area ratio can be selected from **Figure 5**, whereas the nozzle throat diameter is obtained from **Figure 7**. The heat transfer areas of the condenser and the evaporator can be obtained from **Figures 8** and **10**, respectively. Finally, the performances, which are the ejector entrainment ratio and the system COP, can be predicted using **Figures 4** and **6**, respectively.

Table 3 Selection criteria and the procedure to the obtain component sizes.

Procedure	Parameters	Data or Results
1. Define the initial conditions	- Refrigerating capacity	3.5 kW
	- Refrigerant	Water
	- Operating conditions	
	- Generator temperature (T_G)	120 °C
	- Condenser temperature (T_C)	30 °C
	- Evaporator temperature (T_E)	10 °C
2. Determine the component sizes		
- Ejector	- **Figures 6** and **8**	
	- Area ratio (A_R)	59.32
	- Nozzle throat dia. (D_{th})	3.9 mm
- Condenser	- **Figure 9**	
	- Heat transfer area	7.4 m^2
- Evaporator	- **Figure 11**	
	- Heat transfer area	4.6 m^2
3. Determine the system performance	- **Figures 5** and **7**	
	- Entrainment ratio (Rm)	0.7
	- COP	0.65

Table 4 shows the results of 4 different cases with identical refrigerating capacity (3.5 kW) but different operating conditions. This table validates that the analyses in sections 2 and 3 and give reasonable results and significantly confirm the effect of the operating conditions on the component size and the system performances. The system that runs at a low condensing temperature (T_C) (system 1) will provide a high COP; however, its condenser must be bigger than that used with a higher T_C (system 2), whereas the required size of the ejector will also vary. This result implies that when one wants to use a high COP system, one must accept the higher initial cost because of the bigger condenser. A system with a low evaporation temperature (T_E) (system 4) will give a lower COP than the same system with a higher T_E (system 3). However, the evaporator can be smaller, which reduces the equipment cost.

When the generator temperature (T_G) is varied (systems 3 and 4), the ejector characteristics are significantly changed, including the system COP. Changing T_G does not significantly affect the evaporator and condenser heat transfer areas because they depend on their own operating conditions.

Table 4 Sensitivity analysis on component size due to initial conditions.

System No.	Initial conditions				Obtained results					
					Ejector			System	Heat transfer area (m^2)	
	Capacity (kW)	T_G (°C)	T_C (°C)	T_E (°C)	A_R	D_{th} (mm)	Rm	COP	Condenser	Evaporator
1	3.5	120	30	10	59.32	3.9	0.7	0.65	7.24	4.6
2	3.5	120	40	10	31.23	5	0.38	0.352	2.31	4.6
3	3.5	150	40	10	78.68	2.8	0.6	0.547	2.43	4.6
4	3.5	150	40	5	74.56	3.6	0.36	0.327	2.43	2.62

The example systems and their results in **Table 4** show that the operating conditions (T_G, T_C, and T_E) affect the ejector characteristics, the heat exchanger sizes, and the system COP. To select the best system, one may have to sacrifice higher equipment costs and operate under more difficult conditions.

Furthermore, the CFD is used to simulate the flow characteristics of the ejectors (Systems 1 to 4). **Figure 11** shows the validation of the entrainment ratio between the 1-D analysis results and CFD results with identical operating conditions (shown in **Table 4**). For this study the ejector geometry is set as axisymmetric and is simulated with the same model set up in Pianthong *et al.*'s study [23]. **Table 5** shows the CFD model set up.

Table 5 CFD model set up.

Simulating program	**FLUENT v.6.3**
Number of nodes	48,000 (Quadrilateral mesh)
Solving method	Couple implicit
Solving equation	Energy equation
Turbulent model	Realizable k - ε
Working fluid	Water vapour
Fluid property	Ideal gas

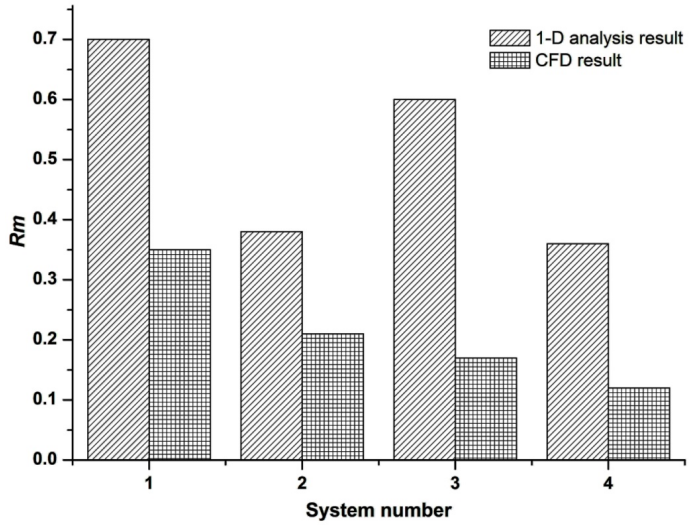

Figure 11 Validation of the entrainment ratio.

Figure 11 reveals that the entrainment ratio of the CFD result is lower than that of the 1-D analysis results. The deviation of entrainment ratio between the 1-D analysis results and CFD result of the systems 1, 2, 3 and 4 are 49.54, 44.86, 72.41 and 65.82 %, respectively. The reason for the deviation is the mathematical model can not exactly predict what the flow characteristics inside the ejector, such as mixing process, over or under expanded wave, diamond wave position and shocking position etc, while the CFD method takes these into account. These flow characteristics are importance factors directly affecting ejector performance, especially the entrainment ratio.

Pianthong *et al*. [23] found that the entrainment ratio and critical back pressure from CFD results are slightly different from the experimental results, approximately 5 %. Furthermore, Rusly *et al*. [20] simulated the flow in an ejector by CFD. It found that, the CFD results more closely match the experimental results than the one-dimensional analysis. It has been shown that CFD is extremely good for predicting the flow characteristics in an ejector. Therefore, for ejector design, when you achieve the ejector geometry from the mathematical model. You have to use the CFD to predict its performance.

Conclusions

This study analyzes the operating condition effects on ejector characteristics, component sizes, and system performance. The specific case that is investigated has a refrigeration capacity of 3.5 kW and uses water as the refrigerant. The operating condition ranges are: 120 - 150 °C for the generator temperature, 30 - 40 °C for the condenser temperature, and 5 - 10 °C for the evaporator temperature. **Figures 4 - 10** can be directly applied to the design or to select the system that works in similar ranges of initial conditions as this specific case. Otherwise, for different conditions, the associated equations, which are presented in this paper, can be used to estimate the component sizes and the system performance. A sensitivity analysis of the component sizes due to the initial conditions from four different systems is discussed. This analysis can be a general guide and good example for the design and construction of facilities or experimental test rigs.

From this study, the major results can be summarized as follows.

- The size and the performance of the system depend on its operating conditions.
- The generator and the evaporator temperatures are directly proportional to the entrainment ratio, the area ratio and the COP. However, they are inversely proportional to the primary nozzle throat diameter.

- The condenser temperature is inversely proportional to the entrainment ratio, the area ratio, and the COP. However, it is directly proportional to the primary nozzle throat diameter.
- For the condenser, the important factor that strongly affects its heat transfer area is the condenser temperature.
- The heat transfer area of the evaporator is increased when the refrigeration capacity and the evaporator temperature increase.
- The system that operates at a lower condenser temperature provides a higher COP, but a larger condenser is required.
- The system that operates at a lower evaporator temperature provides a lower COP, and a smaller evaporator can be used.
- The variation of the generator temperature strongly affects the system performance, whereas the heat exchanger size is only slightly affected.
- Although, the ejector design method using the 1-D analysis in graphical form is simple and quick to employ, its error is relatively high. Therefore the CFD simulation and appropriate tolerance should be considered when one wants to build such a system.

Acknowledgements

The first author would like to thank the Office of the Higher Education Commission, Thailand for support by a grant fund under the program Strategic Scholarships for Frontier Research Network for the Ph.D. Program Thai Doctoral degree for this research. Also, financial support from the National Research Council of Thailand (NRCT) through Ubon Ratchathani University research grant is gratefully acknowledged.

References

[1] S Aphornratana and IW Eames. A small capacity steam-ejector refrigerator: experimental investigation of a system using ejector with movable primary nozzle. *Int. J. Refrig.* 1997; **20**, 352-8.
[2] S Elbel. Historical and present developments of ejector refrigeration systems with emphasis on transcritical carbon dioxide air-conditioning applications. *Int. J. Refrig*. 2011; **34**, 1545-61.
[3] JH Keenan and PE Neuman. A simple air ejector. *T. ASME J. Appl. Mech.* 1942; **64**, 75-81.
[4] IW Eames. A new prescription for design of supersonic jet pump: Constant Rate of Momentum Change Method. *Appl. Therm. Eng.* 2002; **22**, 121-31.
[5] A Milazzo and A Rocchetti. Modelling of ejector chillers with steam and other working fluids. *Int. J. Refrig*. 2015; **57**, 277-87.
[6] A Dahmani, Z Aidoun and N Galanis. Optimum design of ejector refrigeration systems with environmentally benign fluids. *Int. J. Therm. Sci*. 2011; **50**, 1562-72.
[7] A Khalil, M Fatouh and E Elgendy. Ejector design and theoretical study of R134a ejector refrigeration cycle. *Int. J. Refrig*. 2011; **34**, 1684-98.
[8] G Grazzini, A Milazzo and D Pagnini. Design of ejector cycle refrigeration system. *Energ. Convers. Manag*. 2012; **54**, 38-46.
[9] BJ Huang, JM Chang, VA Petrenko and KB Zhuk. A solar ejector cooling system using refrigerant R141b. *Sol. Energy*. 1998; **64**, 223-6.
[10] T Sankarlal and A Mani. Experimental studies on an ammonia ejector refrigeration system. *Int. Commun. Heat Mass.* 2006; **33**, 224-30.
[11] J Chen, H Havtun and B Palm. Investigation of ejectors in refrigeration system: Optimum performance evaluation and ejector area ratios perspectives. *Appl. Therm. Eng*. 2014; **64**, 182-91.
[12] A Selvaraju and A Mani. Analysis of a vapour ejector refrigeration system with environment friendly refrigerants. *Appl. Therm. Eng*. 2004; **24**, 827-38.
[13] N Ruangtrakoon, S Aphornratana and T Sriveerakul. Experimental studies of a steam jet refrigeration cycle: Effect of the primary nozzle geometries to system performance. *Exp. Therm. Fluid Sci*. 2011; **35**, 676-83.

[14] R Yapıcı and CC Yetisen. Experimental study on ejector refrigeration system powered by low grade heat. *Energ. Convers. Manag*. 2007; **48**, 1560-8.
[15] RH Yen, BJ Huang, CY Chen, TY Shiu, CW Cheng and SS Chen. Performance optimization for a variable throat ejector in a solar refrigeration system. *Int. J. Refrig*. 2013; **36**, 1512-20.
[16] D Butrymowicz, K Śmierciew, J Karwacki and J Gagan. Experimental investigations of low-temperature driven ejection refrigeration cycle operating with isobutene. *Int. J. Refrig*. 2014; **39**, 196-209.
[17] DW Sun. Variable geometry ejectors and their applications in ejector refrigeration system. *Energy* 1996; **21**, 919-29.
[18] ED Rogdakis and GK Alexis. Investigation of ejector design at optimum operating condition. *Energ. Convers. Manag*. 2000; **41**, 1841-9.
[19] GK Alexis. Estimation of ejector's main cross sections in steam-ejector refrigeration system. *Appl. Therm. Eng.* 2004; **24**, 2657-63.
[20] E Rusly, L Aye, WWS Charters and A Ooi. CFD analysis of ejector in a combined ejector cooling system. *Int. J. Refrig*. 2005; **28**, 1092-101.
[21] T Sriveerakul, S Aphornratana and K Chunnanond. Performance prediction of steam ejector using computational fluid dynamics: Part 1. Validation of the CFD result. *Int. J. Therm. Sci*. 2007; **46**, 812-22.
[22] T Sriveerakul, S Aphornratana and K Chunnanond. Performance prediction of steam ejector using computational fluid dynamics: Part 2. Flow structure of a steam ejector influenced by operating pressures and geometries. *Int. J. Therm. Sci*. 2007; **46**, 823-33.
[23] K Pianthong, W Seehanam, M Behnia, T Sriveerakul and S Aphornratana. Investigation and improvement of ejector refrigeration system using computational fluid dynamics technique. *Energ. Convers. Manag.* 2007; **48**, 2556-64.
[24] RL Yadav and AW Patwardhan. Design aspects of ejectors: Effects of suction chamber geometry. *Chem. Eng. Sci.* 2008; **63**, 3886-97.
[25] MK Ji, T Utomo, JS Woo, YH Lee, HM Jeong and HS Chung. CFD investigation on the flow structure inside thermo vapor compressor. *Energy* 2010; **35**, 2694-702.
[26] N Ruangtrakoon, T Thongtip, S Aphornratana and T Sriveerakul. CFD simulation on the effect of primary nozzle geometries for a steam ejector in refrigeration cycle. *Int. J. Therm. Sci*. 2013; **63**, 133-45.
[27] Engineering Sciences Data Unit. *Ejector and Jet Pumpdesign for Steam Driven Flow*. London, 1986.
[28] C Saengmanee and K Pianthong. Design of a steam ejector by co-operating the ESDU design method and CFD simulation. *In*: Proceeding of the 1st TSME International Conference on Mechanical Engineering, Ubon Ratchathani, Thailand, 2010.
[29] DQ Kern. *Process Heat Transfer*. McGraw-Hill, Singapore, 1988.
[30] S KakaÇ and H Liu. *Heat Exchanger: Selection, Rating and Thermal Design*. CRC Press, USA, 2002.
[31] J Yu and Z Du. Theoretical study of a transcritical ejector refrigeration cycle with refrigerant R143a. *Renew. Energ.* 2010; **35**, 2034-9.